Oxygen isotope variations in Paleogene volcanic rocks from southern New Mexico: Insight on crustal contamination and magmatic sources

M. Hoffman and G.S. Michelfelder, 2018, pp. 189-196

in:

Las Cruces Country III, Mack, Greg H.; Hampton, Brian A.; Ramos, Frank C.; Witcher, James C.; Ulmer-Scholle, Dana S., New Mexico Geological Society 69th Annual Fall Field Conference Guidebook, 218 p.

This page is intentionally left blank to maintain order of facing pages.

New Mexico Geological Society Guidebook, 69th Field Conference, Las Cruces Country III, 2018, p. 189-196.

OXYGEN ISOTOPE VARIATIONS IN PALEOGENE VOLCANIC ROCKS FROM SOUTHERN NEW MEXICO: INSIGHT ON CRUSTAL CONTAMINATION AND MAGMATIC SOURCES

Max Hoffman and Gary S. Michelfelder*

Department of Geography, Geology and Planning, Missouri State University, 901 S. National Ave, Springfield, MO 65897, *garymichelfelder@missouristate.edu

Abstract—This study reports oxygen isotope values determined by laser fluorination of mineral separates from basalt through rhyolite composition volcanic rocks erupted from the Rubio Peak and Bell Top formations and the Uvas Volcanic Field. Plagioclase phenocrysts from the Uvas Basalts are altered and have $\delta^{18}O$ values of 12.87‰. Pyroxene phenocrysts from the basalts are considered magmatic with $\delta^{18}O$ values of 4.29–5.64‰; quartz contains $\delta^{18}O$ values of 2.10–7.52‰ and is only found as amygdule filling crystals. Phenocrysts from the Rubio Peak Formation basalts and andesites contain $\delta^{18}O$ values of 4.88-5.40‰. Two rhyolite samples from the Bell Top Formation are ash flow tuffs from the Kneeling Nun Tuff and Cooney Canyon Tuff. Plagioclase and quartz phenocryst $\delta^{18}O$ values are restricted, ranging from 6.69–6.73‰ and 8.01–8.23‰, respectively. Biotite phenocrysts from these samples exhibit a greater range in $\delta^{18}O$ values, from 5.21–6.18‰. Calculated magmatic $\delta^{18}O$ values for the Uvas basalts and Rubio Peak andesites range between 6.12 and 6.40‰ corresponding to fractional crystallization of a primary mantle melt, while Bell Top Formation volcanic rocks exhibit higher $\delta^{18}O$ magmatic value of 8.60‰, representing partial melting of a granitic composition crustal source.

INTRODUCTION

Determining magmatic sources and quantifying components during magma differentiation in arc magmas is fundamental for creating realistic models of magma generation and evolution (Borisova et al., 2016; Underwood and Clynne, 2017; Bucholz et al., 2017). Identifying the sources of near-primary or parental mafic mantle magma interacting with continental crust is difficult using trace element and radiogenic isotope compositions alone due to the dramatic compositional changes from small volumes of crustal contamination (e.g., Lackey et al., 2005; Feeley et al., 2008). Oxygen isotope values of igneous minerals and volcanic rocks yield information about the degree and source of partial melting of mantle material producing parental melts, subsequent crustal contamination, and volumes of magma involved in magma evolution (Bucholz et al., 2017).

The complex tectonic history recorded in igneous rocks in southern New Mexico have created a compositionally diverse continental crust, with each component containing a unique geochemical signature. Assessment of magmatic sources of young southern New Mexico igneous rocks commonly employed radiogenic isotopic systems (e.g., Sr and Nd). As a result, it is often difficult to determine primary magma composition due to small compositional contrasts between the magmas and the young arc-related rocks they intrude (Karlstrom et al., 2004; Amato et al., 2008, 2012). Wall rocks can be compositionally identical to plutonic and volcanic rocks from previous eruptive episodes through crustal hybridization in arc settings (Michelfelder et al., 2013). Models of crustal evolution and magma source variation have characterized the physical and chemical processes that affect magma composition and provides limits to differentiation models of open crustal magmatic systems in southern New Mexico. McMillan et al. (2000) suggests that Eocene magmas assimilated both upper and lower crustal components, while Oligocene and late Cenozoic lavas were limited to lower crustal input. This suggests that the crust was thermally matured from early Eocene magmatism in southern New Mexico (Davis and Hawkesworth, 1994, 1995; McMillan et al., 2000).

In this paper, we build on existing age, petrological and compositional studies of volcanic rocks erupted prior to, during, and post ignimbrite flare-up, which comprises the majority of volcanic rock volumes in southern New Mexico. We focus our efforts on three units spanning approximately 10 Ma: the Rubio Peak Formation (51–36 Ma), The Bell Top Formation (36–28 Ma) and the Uvas Volcanic Field (28–25 Ma; McMillan, 1998; McMillan et al., 2000; Rentz et al., in press); through a focused study of oxygen isotope values of mineral separates. These data are used to present a model to evaluate the proportions of mantle versus crustal sources/components as a function of time as space. We present the first oxygen isotope values for volcanic rocks from southern New Mexico and combine these data with whole-rock major- and trace element and radiogenic isotopic data. Collectively, these data allow for southern New Mexico to serve as a case study to better understand the major shift from continental arc magmatism to Rio Grande rifting.

GEOLOGICAL AND PETROLOGICAL BACKGROUND

The styles of volcanism in southern New Mexico (Fig. 1) and the composition of the magmas erupted changed significantly with the end of Laramide subduction. In general, Laramide volcanism in the Basin and Range area, including southern New Mexico, began with the eruption of intermediate to silicic com-

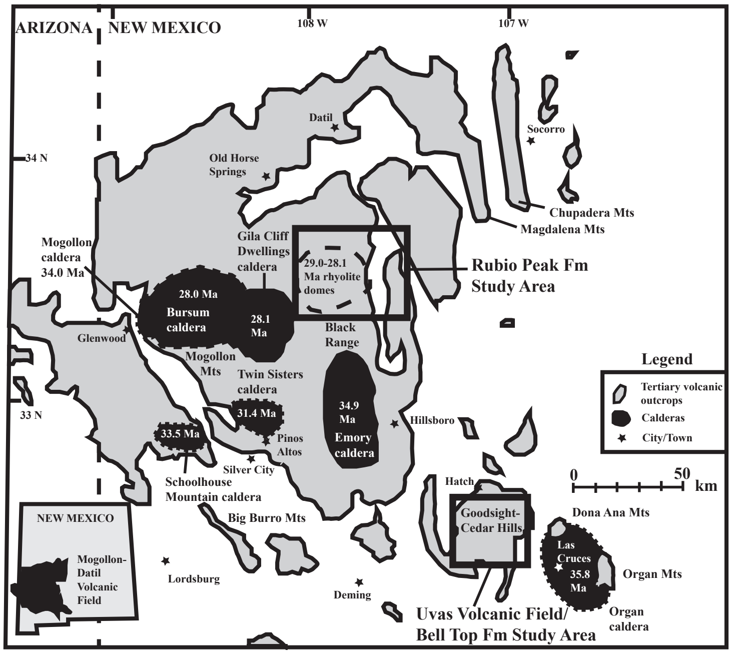

FIGURE 1. Simplified geologic map of southern New Mexico showing late Eocene to Oligocene volcanic rock outcrops and caldera locations. Dashed outlined calderas indicate calderas that are equivalent age to the Bell Top Formation volcanic rocks but are not included in this study. Black boxes indicate location of the study areas of the Rubio Peak Formation and the Uvas Volcanic Field. Modified from McIntosh et al. (1992).

position ignimbrites. Post-ignimbrite extension is recorded by a period of syntectonic basin fill that provides evidence to the timing of volcanism with respect to extension (Best and Christiansen, 1991; Gans and Bohrson, 1998). A decrease in extension rate and switch to alkalic, dominantly mafic, volcanism in southern New Mexico resulted from an increase in crustal density and the intrusion of mafic magma (Glazner and Ussler, 1989).

Rubio Peak volcanic rocks range in age from 45–37.6 Ma and represent the initiation of volcanic activity in the Mogollon Datil Volcanic Field (MDVF; Davis et al., 1993; Davis and Hawkesworth, 1994). The largest volume of Rubio Peak rocks are broadly "arc-like" in composition and are hornblende-bearing, high-K andesite ranging in SiO_2 from 58–62 wt% (Davis and Hawkesworth, 1994, 1995; McMillan et al., 2000). A distinct and abrupt change in composition and eruptive style marks the boundary between volcanic rocks of the Rubio Peak Formation and volcanic rocks of the Bell Top Formation (Fig. 1). High-precision $^{40}Ar/^{39}Ar$ ages of ash-flow sheets comprising the silicic end member volcanic rocks place this period of activity between 36.2 and 28.6 Ma in southern New Mexico (McIntosh et al., 1992). The Bell Top Formation is made up of bimodal basaltic dikes and rhyolite ignimbrites erupted during peak flare-up of the Mogollon Datil Volcanic Field. Silicic pyroclastic volcanism ended at ~28.5 Ma in southern New Mexico, but persisted in south-central New Mexico until ~24 Ma (McIntosh et al., 1992). Overlying the ignimbrites in southern New Mexico are calc-alkline basalt, basaltic andesite, and andesite lava flows associated with the Uvas Volcanic Field (UVF; Fig. 1; McMillan et al., 2000). Around 25 Ma, volcanism in southern New Mexico ceased until around 10 Ma. The youngest volcanic rocks in New Mexico are alkaline basalts associated with extension of the Rio Grande Rift (McMillan et al., 2000; McMillan, 2004; Michelfelder and McMillan, 2012).

METHODS

Major element oxide analyses were obtained by X-ray fluorescence (XRF) spectrometry (Johnson et al., 1999) and the rare earth elements (REE) and select trace elements were analyzed by inductively coupled plasma-mass spectrometry (ICP-MS) at the Peter Hooper GeoAnalytical Laboratory at Washington State University (Jarvis, 1988). Pb, Nd, and Sr isotope ratios on whole rock powders were determined by the methods described in Ramos and Reid (2005) at New Mexico State University. Oxygen isotope measurements were obtained and analyzed in the GeoAnalytical Laboratory at Washington State University by the method of Takeuchi and Larson (2005). One standard, UWG-2 garnet (Valley et al., 1995) was measured with a difference of 0.2‰ from the published value of 5.89‰ relative to Vienna standard mean ocean water (VSMOW). Data is reported in per mille using standard delta notation relative to VSMOW.

RESULTS

Table 1 summarizes $\delta^{18}O$ values for nine samples, four from the Uvas basalts, three from the Rubio Peak Formation, and two

TABLE 1. Oxygen isotope values of mineral separates from volcanic rocks included in this study.

	Uvas Volcanic Field				Rubio Peak Formation			Bell Top Formation	
	UV 2	UV 3	UV 4	UV 5	TRP 1	TRP 2	TRP 6	MO 09	TRP 3
Latutude	32.52	32.52	32.52	32.52	33.25	33.25	33.48	33.83	33.29
Longitude	-107.2	-107.2	-107.2	-107.2	-107.7	-107.7	-107.77	-108.83	-107.63
$\delta^{18}O_{qtz}$	7.52			2.10				8.23	8.01
$\delta^{18}O_{pyx}$			5.64	4.29	5.16	4.88	5.22		
$\delta^{18}O_{plag}$		12.87*					5.40	6.69	6.73
$\delta^{18}O_{mag}$	11.03								
$\delta^{18}O_{bio}$								5.21	4.82

Notes *weathered sample

from the Bell Top Formation (represented by the Kneeling Nun Tuff, and the Cooney Canyon Member of the Cooney Formation). The focus of this manuscript is on oxygen isotope values of previously described volcanic rocks from southern New Mexico. Whole-rock major- and trace element concentrations and Sr, Nd, and Pb isotopic ratios are included in Tables 2 and 3, but are not discussed other than to define volcanic rock types and compare our data to the data of McMillan et al. (2000) and Davis

TABLE 2. Major- and trace element whole rock data for volcanic rocks included in this study.

	Bearwallow Mountain Andesite					Bell Top Formation			Rubio Peak Formation			
	APA-3	**PP-010**	**PP-4**	**SFH2**	**MO-08**	**MO-01**	**MO-09**	**MO-12**	**TRP-1**	**TRP-2**	**TRP-4**	**TRP-6**
Age	~24 Ma	~24 Ma	~24 Ma	~24 Ma	25 Ma	3 Ma	33.1 Ma	31.8 Ma	36 Ma	36 Ma	36 Ma	36 Ma
Latitude	33.73	33.63	33.71	33.15	33.38	33.38	33.38	33.38	33.25	33.25	33.31	33.48
Longitude	-108.96	-108.92	-108.91	-109.03	-108.83	-108.83	-108.83	-108.83	-107.7	-107.7	-107.64	-107.77
SiO_2	53.58	48.57	57.36	59.17	45.84	66.22	73.36	67.29	58.80	60.39	58.01	51.00
TiO_2	1.324	1.979	0.857	1.008	1.930	0.622	0.323	0.452	0.965	0.812	0.956	0.952
Al_2O_3	16.18	17.65	18.38	16.43	16.30	13.75	13.56	13.99	16.26	17.06	17.47	15.80
FeO*	8.00	10.46	5.68	6.13	9.57	4.81	1.81	3.81	5.78	4.92	6.01	6.74
MnO	0.124	0.156	0.090	0.105	0.143	0.046	0.125	0.065	0.080	0.088	0.078	0.100
MgO	6.18	4.19	2.44	3.16	3.97	2.65	1.28	1.12	3.39	2.54	2.58	4.42
CaO	7.17	9.79	6.66	5.72	7.60	1.48	0.35	1.78	4.51	5.15	5.97	7.10
Na_2O	3.55	2.99	3.72	3.57	2.58	2.34	1.37	3.00	5.23	3.86	4.21	3.62
K_2O	2.54	1.07	2.37	2.67	2.46	2.26	4.75	4.87	1.63	3.08	2.05	1.81
P_2O_5	0.520	0.303	0.240	0.346	0.388	0.142	0.042	0.157	0.302	0.264	0.288	0.270
Sum	99.16	97.15	97.79	98.32	90.78	94.33	96.96	96.54	96.95	98.18	97.61	91.81
LOI %	0.71	2.40	0.56	1.59	9.06	4.67	2.38	2.94	2.96	1.64	2.20	7.88
Ni	198	35	19	41	40	25	4	7	42	31	57	50
Cr	310	14	20	43	47	20	3	5	72	63	87	126
V	173	244	137	123	228	113	14	108	137	101	116	134
Ga	19	17	20	20	20	17	16	17	18	20	21	19
Cu	61	40	29	42	46	57	12	29	13	105	36	17
Zn	84	87	67	81	98	62	70	65	82	71	79	69
La	34.85	20.20	31.42	50.24	26.06	23.86	42.50	32.92	30.77	32.34	32.07	23.43
Ce	72.51	42.01	65.91	101.75	54.99	47.96	83.74	67.18	61.14	64.11	64.88	47.93
Pr	9.01	5.31	8.08	12.13	6.98	5.88	9.79	7.84	7.44	7.59	7.85	5.98
Nd	35.39	21.92	31.44	46.35	29.00	22.91	34.80	29.20	28.85	29.04	30.41	23.86
Sm	6.71	4.86	6.44	8.83	6.16	4.72	6.37	5.43	5.63	5.35	5.89	4.73
Eu	1.97	1.70	1.56	2.03	1.79	1.07	1.11	1.10	1.73	1.67	1.62	1.79
Gd	5.55	4.77	5.71	7.40	5.73	4.26	4.98	4.40	4.28	4.08	4.69	3.78
Tb	0.85	0.76	0.93	1.14	0.90	0.72	0.86	0.73	0.63	0.60	0.68	0.56
Dy	4.72	4.59	5.77	6.58	5.18	4.61	5.49	4.45	3.49	3.13	3.84	3.10
Ho	0.92	0.92	1.16	1.29	1.01	0.94	1.17	0.91	0.65	0.58	0.76	0.60
Er	2.30	2.38	3.09	3.41	2.62	2.61	3.53	2.59	1.67	1.50	1.97	1.52
Tm	0.33	0.34	0.45	0.49	0.37	0.40	0.57	0.40	0.24	0.21	0.27	0.21
Yb	2.00	2.05	2.80	2.97	2.27	2.47	3.91	2.58	1.41	1.29	1.65	1.24
Lu	0.30	0.30	0.43	0.44	0.35	0.38	0.66	0.40	0.20	0.20	0.26	0.19
Ba	1058	314	685	1080	102	289	1817	339	988	1226	847	820
Th	4.62	2.42	8.88	7.09	4.05	10.23	16.26	7.96	4.76	6.50	4.13	2.96
Nb	11.46	19.73	7.43	12.18	25.36	7.15	12.08	7.60	8.29	10.48	7.32	6.28
Yb	22.87	22.62	29.87	33.67	25.17	24.46	32.23	25.18	16.41	15.13	20.23	14.64
Hf	5.63	3.18	5.73	7.60	4.21	5.30	7.20	5.08	4.41	5.14	4.78	3.21
Ta	0.69	1.31	0.52	0.70	1.59	0.55	1.04	0.53	0.52	0.73	0.44	0.41
U	0.81	0.62	1.84	1.11	0.97	2.89	3.50	2.92	0.87	1.53	0.72	0.46
Pb	11.06	3.09	12.38	14.13	9.34	9.44	49.93	26.26	10.81	12.11	8.04	6.98
Rb	41.6	19.6	75.5	79.3	143.5	117.0	157.2	265.0	32.6	68.1	41.7	42.5
Cs	0.37	0.12	1.50	1.87	16.33	14.43	14.36	7.63	0.29	0.59	0.75	4.41
Sr	719	489	603	590	495	172	176	150	781	895	773	657
Sc	18.3	22.5	14.0	14.3	24.6	12.7	3.7	7.3	13.5	9.1	12.9	15.7
Zr	222	127	210	305	167	192	259	181	170	195	184	126

TABLE 3. Whole rock Sr, Nd, and Pb isotope ratios of select volcanic rocks included in this study.

	Uvas Volcanic Field		Rubio Peak Fm.	Bell Top Fm.
Sample	**UV-1**	**UV-5**	**TRP6**	**CC-01**
Age	**28 Ma**	**28 Ma**	**36 Ma**	**31.8 Ma**
$^{87}Sr/^{86}Sr_m$	0.705075	0.704767	0.706046	0.715022
Error	*0.000010*	*0.000018*	*0.000012*	*0.000008*
$^{87}Sr/^{86}Sr_i$	0.7050159	0.7047079	0.7059519	0.710987
$^{143}Nd/^{144}Nd_m$	0.512361	0.512591	0.512339	0.512197
Error	*0.000004*	*0.000005*	*0.000006*	*0.000005*
$^{143}Nd/^{144}Nd_i$	0.512347	0.512577	0.512311	0.5121703
ε_{Nd}	-5.0	-0.5	-5.5	-8.3
$^{206}Pb/^{204}Pb$	17.209	17.587	17.537	18.430
Error	*0.001*	*0.001*	*0.001*	*0.001*
$^{207}Pb/^{204}Pb$	15.424	15.466	15.467	15.561
Error	*0.001*	*0.001*	*0.001*	*0.001*
$^{208}Pb/^{204}Pb$	37.210	37.733	37.658	38.474
Error	*0.002*	*0.003*	*0.002*	*0.002*

and Hawkesworth (1994, 1995). Rubio Peak Formation volcanic rocks represent a continuous liquid line of decent from basalt to dacite with SiO_2 ranging from 46.8 to 64.4 wt% (Table 2; Davis and Hawkesworth, 1994; McMillan et al., 2000). Ratios of Ba/Zr and Sr/Y ranges from 4.1–8.1 and 8.6–14.0 respectively (Fig. 2). Sr/Y ratios decrease with increasing Y content. Eu anomaly are slightly positive to moderately negative (0.64–1.20; ratios close to one are considered not to have an anomaly). Sr isotope ratios from this study and those included in the studies of Davis and Hawkesworth, (1994; 1995) and McMillan et al. (2000) range from 0.704433 to 0.706880 and Nd isotope ratios between 0.512361 and 0.512430. $^{208}Pb/^{204}Pb$ range between 37.09 and 37.94, $^{207}Pb/^{204}Pb$ range between 15.40 and 15.52 and $^{206}Pb/^{204}Pb$ range between 17.04 and 17.95 (Fig. 3).

Cooney Formation and Kneeling Nun Tuff samples are rhyolite ash flow tuffs ranging in SiO_2 between 72 to75 wt%. Rhyolites have consistently lower Ba/Zr, Sr/Y and Eu anomalies compared to the basalts and andesites, but similar Y contents and Nb/Zr ratios. Sr, Nd and Pb isotope ratios contain more crustal (more radiogenic) signatures (Fig. 3).

Uvas Volcanic Field lavas range from basalt to basaltic andesite and are geochemically described in McMillan et al. (2000) and illustrated in Figure 2. New Sr, Nd and Pb isotopic data for two basalts are presented in Figure 3. Sr and Nd isotopic ratios are within the range observed by McMillan et al. (2000) with new $^{87}Sr/^{86}Sr$ ratios of 0.704767±10 and 0.705075±18 and $^{143}Nd/^{144}Nd$ ratios of 0.512361±4 and 0.512591±5. $^{208}Pb/^{204}Pb$ ratios of 37.37 and 38.13, $^{207}Pb/^{204}Pb$ ratios of 15.43 and 15.50 and $^{206}Pb/^{204}Pb$ ratios of 17.32 and 18.08 (Fig. 3). New $^{208}Pb/^{204}Pb$ range between 37.21 and 37.73, $^{207}Pb/^{204}Pb$ range between 15.42 and 15.47 and $^{206}Pb/^{204}Pb$ range between 17.21 and 17.59 (Fig. 3; Table 3).

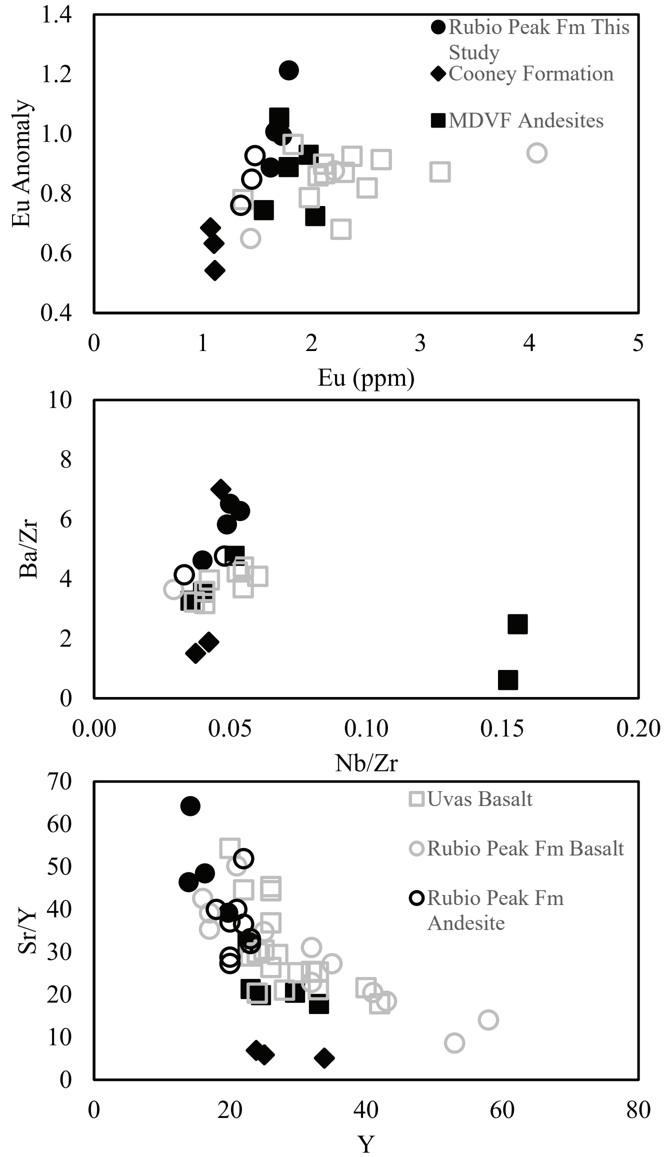

FIGURE 2. Whole rock trace element ratios versus SiO_2 or trace element content of volcanic rocks from southern New Mexico. Additional Rubio Peak and Uvas basalt and andesite data from McMillan et al. (2000) and Davis and Hawkesworth (1994, 1995).

OXYGEN ISOTOPE VALUES OF MINERAL SEPARATES

Plagioclase from the Rubio Peak Formation (TRP) ranges from 5.4–6.73‰ and are within the normal range for unaltered silicic igneous rocks as defined by Taylor (1968; Fig. 4). Plagioclase from the Uvas Volcanic Field (UVF) andesites are much higher (one samples 12.87‰). UVF plagioclase mineral separates visually appeared altered and the high $\delta^{18}O$ values confirm this observation. Pyroxene separates from both the TRP (4.88–5.28‰) and UVF (4.29–5.64‰) are at the lower range of normal unaltered silicic igneous rocks (Taylor, 1968; Fig. 4). Biotite phenocrysts from the Rubio Peak and the Bell Top Formations are only present in high silica andesites through rhyolites. No biotite was analyzed from the Rubio

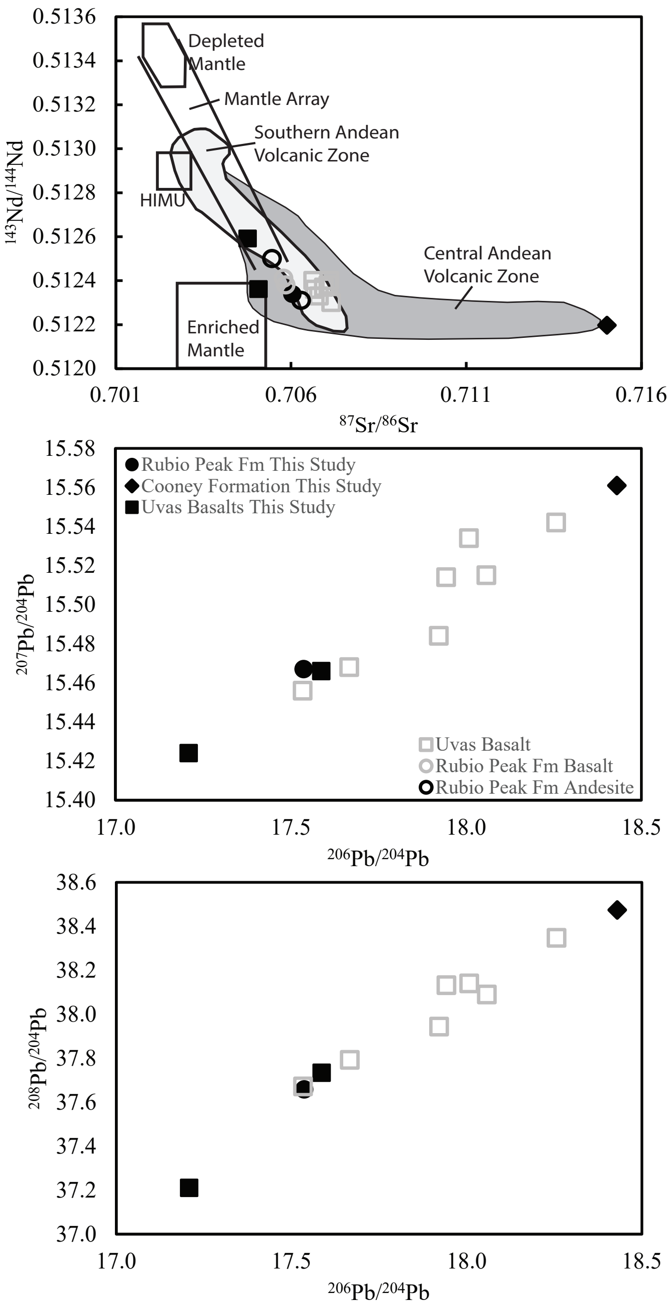

FIGURE 3. Whole rock Sr, Nd and Pb isotopic ratios for Rubio Peak, Uvas Volcanic Field and Mogollon Datil Volcanic field volcanic rocks. Rubio Peak Formation and Uvas Basalt volcanic rock data from McMillan et al. (2000) and Davis and Hawkesworth (1993, 1994). Southern Andean Volcanic Zone field from Hickey et al. (1986) and Central Andean Volcanic Zone field from Hildreth and Moorbath (1988).

Peak Formation. Bell Top biotite ranges from 4.82 to 6.18‰. Quartz phenocrysts were observed in the Bell Top Formation ash flows and two basalts from the Uvas Volcanic Field. All quartz phenocrysts are subhedral to anhedral and exhibit dissolution textures. Uvas basalt quartz exhibits a wide range of $\delta^{18}O$ values of 2.10 to 7.52‰. Bell Top quartz phenocrysts are more consistent with $\delta^{18}O$ values from 8.01 to 8.23‰.

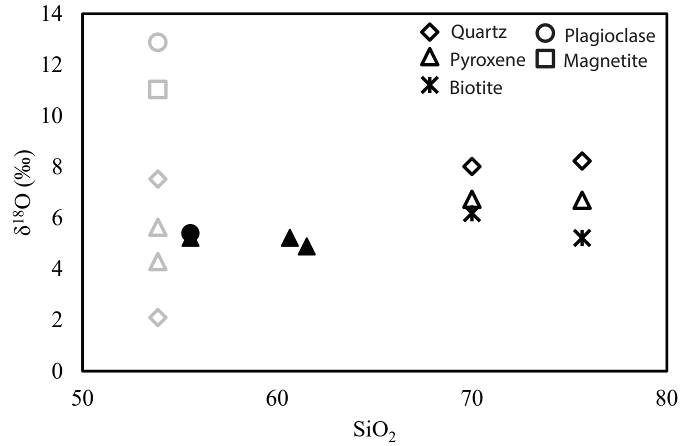

FIGURE 4. Oxygen isotope values of mineral separates versus whole rock SiO_2 content from Rubio Peak and Uvas lava flows and Bell Top Formation. Open grey symbols are Uvas volcanic rocks, closed black symbols are Rubio Peak volcanic rocks and open black symbols are Cooney and Kneeling Nun ash flow tuffs representing the Bell Top Formation. SiO_2 contents for Uvas basalts from McMillan et al. (2000).

DISCUSSION

Effects of alteration

Given that the aim of this study is to use oxygen isotope values to constrain the petrogenesis of the Rubio Peak Formation and Uvas Volcanic Field mafic and intermediate rocks, it is crucial to understand which, if any, of the measured minerals $\delta^{18}O$ values can be reliably used as a proxy for magma $\delta^{18}O$. This is of particular importance for the Uvas rocks due to petrographic evidence of secondary mineralization of calcite and quartz and Fe-oxide staining in amygdules (Hoffman, 2017).

To investigate the degree of internal O-isotope equilibrium, the $\delta^{18}O$ values of biotite, plagioclase, pyroxene, and quartz are plotted against whole-rock SiO_2 (Fig. 4). Plagioclase, and quartz, all exhibit variability versus whole-rock SiO_2 within a given sample, but plagioclase and quartz are consistently higher in the Uvas basalts compared to pyroxene phenocrysts. High $\delta^{18}O$ values of plagioclase (>7.5‰) are consistent with low-temperature hydrothermal alteration (Taylor, 1968; Fourie and Harris, 2011). The susceptibility of feldspar to alteration is often used to identify post magmatic alteration in rocks as it reflects disequilibrium with more resistant phase such as quartz or pyroxene (Fourie and Harris, 2011). There is no evidence of high temperature alteration which would have lowered $\delta^{18}O$ values of feldspar for all three formations (Taylor, 1968, 1977). Rubio Peak samples are more consistent between all phases and are consistent with equilibrium at magmatic temperatures. Plagioclase $\delta^{18}O$ values are consistent with equilibrium with pyroxene at magmatic temperatures in the Rubio Peak Formation samples. Quartz contains high $\delta^{18}O$ values compared to other phases for andesite and dacite composition samples, but records limited variability of ~0.22‰. Associated disequilibrium textures suggest that silicic samples of the Bell Top Formation which containing quartz have undergone some degree of crustal contamination while basaltic and less silicic andesite samples of the UVF with quartz suggests hydrothermal alteration.

Original magma $\delta^{18}O$: Rubio Peak and Bell Top Formation

The limited variation in pyroxene, plagioclase, and biotite in the Rubio Peak volcanic rocks suggest crystallization from magma(s) having a limited range in $\delta^{18}O$ value (~0.5‰) for the basalt and andesite and a higher range for the dacite (~1.9‰) of the Bell Top. Biotite in these samples may exhibit some degree of hydrous breakdown lowering biotite $\delta^{18}O$ values and increasing the variation exhibited. When biotite is excluded from the $\delta^{18}O$ values, andesite show limited variation (0.06‰ or within analytical error). Using the equation of Lackey et al. (2008) to estimate $\Delta^{18}O_{(WR\text{-}pyroxene)}$ and therefore $\delta^{18}O_{WR}$ values, the magma $\delta^{18}O$ value is between 6.21‰ for the basalt and andesite and 8.6‰ for Bell Top felsic magmas (WR value based on plagioclase for felsic rocks). The differences in estimates of the $\delta^{18}O$ value of the original magmas of the Rubio Peak mafic and intermediate rocks result from uncertainties in fractionation factor, magmatic temperature, and the model used to estimate $\Delta_{pyroxene\text{-}mineral}$ and $\Delta_{pyroxene\text{-}magma}$. Nevertheless, estimates of $\delta^{18}O$ value based on pyroxene and plagioclase for Rubio Peak rocks are broadly consistent and it is concluded that the original magma(s) had average $\delta^{18}O$ value between 6.12 and 6.40‰. Therefore, in the Rubio Peak Formation basalt and intermediate rocks, pyroxene can be used as a proxy for magma $\delta^{18}O$ value; and in Bell Top rocks plagioclase can be a proxy for magma $\delta^{18}O$ value.

Original magma $\delta^{18}O$: Uvas Volcanic Field

Phenocrysts from the Uvas Volcanic Field basalts and andesites are considered to be highly altered with the exception of pyroxene from two basalt lava flows. While SiO_2 content was not measured for Uvas rocks, a robust data set does exist from McMillan et al. (2000). Using an average SiO_2 content of 52.2 wt% SiO_2 suggests that the basalts from the Uvas Volcanic field range in $\delta^{18}O_{WR}$ between 5.1 and 6.45‰. Even when adding the lowest and highest SiO_2 content measured in the UVF, $\delta^{18}O_{WR}$ values range between 4.91 to 6.25‰ and 5.58 to 6.93‰, respectively. In this study, we define normal $\delta^{18}O$ magmas as having an oxygen isotope values consistent with derivation by crystal differentiation from basalt of an arc-mantle source (+5.8±0.2‰). There is overall agreement that differentiation from basalt to rhyolite creates a positive subper mil change in $\delta^{18}O$ value (Fig. 5; and references within the figure). Values below 5.8‰ are considered to be the result of low temperature hydrothermal alteration of these samples. This suggests that the $\delta^{18}O_{pyx}$ value of 5.64 ±0.2‰ from sample UV4 of the Uvas Volcanic Field basalts best represents the magma composition, and therefore, $\delta^{18}O_{WR}$ is 6.25‰.

Oxygen isotope constraints on sources of southern New Mexico magmas

The shaded field in Figure 5 is the 'normal $\delta^{18}O$ array' as suggested by Bindeman et al. (2004) for a closed system undergoing crystal fractionation from a primitive arc basaltic magma with a $\delta^{18}O$ value of ~5.8±0.2‰. There are a variety of $\delta^{18}O_{(melt)}$ trajectories with increasing fractionation of basalt, but the overall increase in $\delta^{18}O$ values average out and yield smooth trends of increasing $\delta^{18}O$ value with increasing SiO_2. Calculated trends, here called normal arrays, plot in the middle, but with high and low natural cited estimates and agree with recent results for ocean islands (Harris et al., 2000; Bindeman et al., 2004). The primitive composition of arc basalt that defines the 'normal array' was selected based on the defining characteristics of McMillan (1998) and McMillan et al. (2000) for subduction modified lithospheric mantle versus asthenospheric mantle and best represents the geochemical compositions of Rubio Peak Formation and Uvas Volcanic Field mafic and intermediate volcanic rocks. The array suggests the fractionation of a high-Mg series subalkaline basalt with crystallization of olivine and plagioclase. High-Al series and alkali-rich series magmas exhibit a similar trend with a wider array of $\delta^{18}O$ values. As illustrated in Figure 5, magmatic $\delta^{18}O$ values calculated from plagioclase and pyroxene phenocrysts for both the UVF and TRP plot along the closed system mantle fractionation field, with some variation. This trend suggests that while the two volcanic suites are separated by ~14 Ma, both systems are dominated by fractional crystallization. Phenocryst and whole-rock $\delta^{18}O$ values plotted versus SiO_2 form a continuous liquid line of decent derived from subduction modified lithospheric mantle basalts, consistent with the previous studies that suggest minimal interaction with continental crust during magma

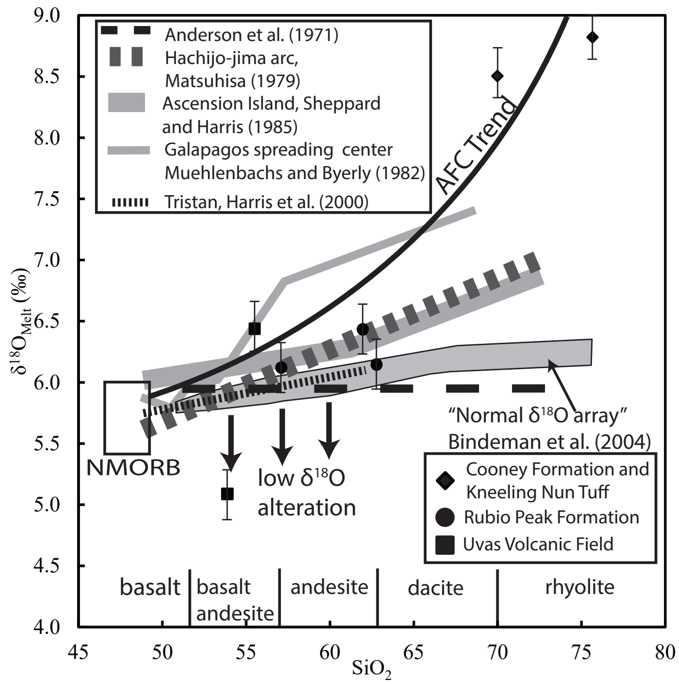

FIGURE 5. Calculated $\delta^{18}O_{WR}$ values of melt as determined by $\Delta^{18}O_{(WR\text{-}mineral)}$ southern New Mexico volcanic rocks versus whole-rock SiO_2 contents. The shaded area is the 'normal $\delta^{18}O$ array' of Bindeman et al. (2004), which depicts modeled oxygen isotope values at a given SiO_2 content resulting from closed-system crystal-liquid fractionation of primitive basaltic magma ($\delta^{18}O$=5.8±0.2‰) under a variety of differentiation conditions and parental magma compositions (Bindeman et al., 2004). Continuous curve labeled 'AFC' schematically illustrates effect of fractional crystallization plus assimilation of heterogeneous, high $\delta^{18}O$ crust on parental magmas.

migration represented by slightly elevated $\delta^{18}O$ values (Davis and Hawkesworth, 1994, McMillan et al., 2000). The more felsic Bell Top rocks contain $\delta^{18}O$ values that plot well above the closed system fractionation trend and are relatively enriched in ^{18}O compared to the little evolved lavas of the TRP and UVF. Therefore, even though the felsic Bell Top volcanic rocks of the Kneeling Nun Tuff and the Cooney Canyon Tuff have trace element and isotopic compositions that fall within the ranges for differentiation of basalt through fractional crystallization, they cannot, as previously argued (Bikerman, 1994; Davis and Hawkesworth, 1995), be explained by direct partial melting of intrusive equivalents of the basaltic and intermediate rocks. Rhyolites of the peak ignimbrite flare-up (Bell Top Fm.) must contain a high $\delta^{18}O$ value crustal component. Furthermore, based on Sr/Y, Rb/Sr, La/Yb and Eu/Eu* ratios, the crustal source for these magmas is suggested to be derived from a more felsic, plagioclase-rich, granitic composition source than the composition of the TRP basalt and andesite compositions used in the fractionation model. The partial melts/contaminant should therefore have $\delta^{18}O$ values and radiogenic isotope values essentially identical to the source due to small bulk mineral-melt fractionations and the consistency of $^{143}Nd/^{144}Nd$ and $^{87}Sr/^{86}Sr$ initial ratios across the region (Fig. 5). Oxygen isotope values of more felsic magmas are therefore considered to be representative of their crustal sources and plot above the 'normal mantle array' and the little evolved basaltic magmas erupted from the TRP. The oxygen isotope data for silicic rocks of the TRP and UVF, therefore provide unequivocal evidence for partial melting of mantle source rocks with andesite contaminated by late Cenozoic subduction modified lithospheric mantle-related lower crust.

CONCLUSIONS

This study shows that more detailed oxygen isotope investigations are need to determine the petrogenic history of igneous rocks in southern New Mexico. Average magma $\delta^{18}O$ values for the Rubio Peak and Uvas basalt and basaltic andesite are 6.21 and 6.25‰, respectively. More felsic magmas of the Bell Top Formation average magma $\delta^{18}O$ values of 8.6‰. Our analysis of mineral separates suggest that basalts from the Uvas Volcanic Field and the Rubio Peak Formation exhibit volumetrically minor amounts of crustal contamination and are derived from subduction modified mantle source. More felsic magmas from the Bell Top Formation are crustal in origin and $\delta^{18}O$ values represent the crustal source. Our data correspond with the conclusions of McMillan (1998) who suggested two distinct subduction modified lithospheric mantle sources evolving during the 10 Ma history of the Mogollon Datil ignimbrite flare-up.

ACKNOWLEDGMENTS

The authors wish to thank Frank Ramos for use of and assistance with the radiogenic isotope analyses at New Mexico State University; Peter Larson, Amber Hasten and the staff at the Geoanalyitical lab at Washington State University for analyzing samples for major and trace element contents and oxygen isotope values. Amber Hoffman and Grant Spoering for assistance in the field collecting samples and measuring stratigraphic sections. Kevin Mickus and Xin Maio for reviewing early versions of this manuscript and serving on the M.S. thesis committee of MH. We thank Damon Bassett and Emily Salings for reviewing the manuscript, and guidebook editors Brian Hampton and Greg Mack for handling this paper during the review process. Support for this work came from grants to GSM and MH from the Graduate College and the Department of Geography, Geology and Planning at Missouri State University.

REFERENCES

Amato, J., Athens, C., McIntosh, W.C., and Peters, L., 2012, U-Pb zircon ages from crustal xenoliths in a Pliocene basalt flow from the southern Rio Grande Rift: Implications for the timing of extension and magmatism: New Mexico Geological Society, Guidebook 63, p. 273-284.

Amato, J.M., Boullion, A.O., Serna, A.M., Sanders, A.E., Farmer, G.L., Gehrels, G.E., and Wooden, J.L., 2008, Evolution of the Mazatzal province and the timing of the Mazatzal orogeny: Insights from U-Pb geochronology and geochemistry of igneous and metasedimentary rocks in southern New Mexico: Geological Society of America Bulletin, v. 120, p. 328-346.

Best, M.G., and Christiansen, E.H., 1991, Limited extension during peak Tertiary volcanism, Great Basin of Nevada and Utah: Journal of Geophysical Research: Solid Earth (1978–2012), v. 96, no. B8, p. 13509-13528.

Bikerman, M., 1994, Are the western Mogollon-Datil mid-Cenozoic ash flows cogenetic? Pearce element ratios and isotopic aspects of the question: New Mexico Geological Society, Guidebook 45, p. 187-192.

Bindeman, I.N., Ponomareva, V.V., Bailey, J.C., and Valley, J.W., 2004, Volcanic arc of Kamchatka: a province with high-delta 18O magma sources and large-scale $^{18}O/^{16}O$ depletion of the upper crust: Geochimica et Cosmochimica Acta, v. 68, p. 841-865.

Borisova, A.Y., Gurenko, A.A., Martel, C., Kouzmanov, K., Cathala, A., Bohrson, W.A., Pratomo, I., and Sumarti, S., 2016, Oxygen isotope heterogeneity of arc magma recorded in plagioclase from the 2010 Merapi eruption (Central Java, Indonesia): Geochimica et Cosmochimica Acta, v. 190, p. 13-34.

Bucholz, C.E., Jagoutz, O., VanTongeren, J.A., Setera, J., and Wang, Z., 2017, Oxygen isotope trajectories of crystallizing melts: Insights from modeling and the plutonic record: Geochimica et Cosmochimica Acta, v. 207, p. 154-184.

Davis, J.M., Elston, W.E., and Hawkesworth, C.J., 1993, Basic and intermediate volcanism of the Mogollon-Datil volcanic field: implications for mid-Tertiary tectonic transitions in southwestern New Mexico, USA: London, Geological Society, Special Publications, v. 76, p. 469-488.

Davis, J.M., and Hawkesworth, C.J., 1994, Early Calc-Alkaline Magmatism in the Mogollon-Datil Volcanic Field, New-Mexico, USA: Journal of the Geological Society, v. 151, p. 825-843.

Davis, J.M., and Hawkesworth, C.J., 1995, Geochemical and Tectonic Transitions in the Evolution of the Mogollon-Datil Volcanic Field, New-Mexico, USA: Chemical Geology, v. 119, p. 31-53.

Feeley, T.C., Clynne, M.A., Winer, G.S., and Grice, W.C., 2008, Oxygen isotope geochemistry of the Lassen Volcanic Center, California: Resolving crustal and mantle contributions to continental arc magmatism: Journal of Petrology, v. 49, p. 971-997.

Fourie, D.S., and Harris, C., 2011, O-isotope study of the Bushveld Complex granites and granophyres: constraints on source composition, and assimilation: Journal of Petrology, v. 52, p. 2221-2242.

Gans, P.B., and Bohrson, W.A., 1998, Suppression of Volcanism during Rapid Extension in the Basin and Range Province, United States: Science, v. 279, no. 5347, p. 66-68.

Glazner, A.F., and Ussler, W., 1989, Crustal Extension, Crustal Density, and the Evolution of Cenozoic Magmatism in the Basin and Range of the Western United-States: Journal of Geophysical Research-Solid Earth and Planets, v. 94, no. B6, p. 7952-7960.

Harris C., Smith H S., and le Roex A.P., 2000. Oxygen isotope composition of phenocrysts from Tristan da Cunha and Gough Island lavas: Variation with fractional crystallization and evidence for assimilation: Contributions to Mineralogy and Petrology, v.138, p. 164–175.

Hickey, R.L., Frey, F.A., Gerlach, D.C., and Lopez-Escobar, L., 1986, Multiple sources for basaltic arc rocks from the southern volcanic zone of the Andes (34–41 S): trace element and isotopic evidence for contributions from subducted oceanic crust, mantle, and continental crust: Journal of Geophysical Research: Solid Earth (1978–2012), v. 91, no. B6, p. 5963-5983.

Hildreth, W., and Moorbath, S., 1988, Crustal Contributions to Arc Magmatism in the Andes of Central Chile: Contributions to Mineralogy and Petrology, v. 98, p. 455-489.

Hoffman, M.L., 2017, The Geochemistry, Petrology and Volcanic Structures of the Uvas Volcanic Field and Rubio Peak Formation of South-Central New Mexico [M.S. thesis]: Springfield, Missouri State University, 91 p.

Jarvis, K.E., 1988, Inductively Coupled Plasma Mass-Spectrometry - a New Technique for the Rapid or Ultra-Trace Level Determination of the Rare-Earth Elements in Geological-Materials: Chemical Geology, v. 68, p. 31-39.

Johnson, D.M., Hooper P.R., and Conrey, R.M., 1999, GeoAnalytical Lab, Washington State University: Advances in X-ray Analysis, v. 41, p. 843-867.

Karlstrom, K.E., Amato, J., Williams, M.L., Heizler, M., Shaw, C., Read, A., Bauer, P., Mack, G., and Giles, K., 2004, Proterozoic tectonic evolution of the New Mexico region: A synthesis, *in* Mack, G.H. and Giles, K.A, eds., The Geology of New Mexico: A Geologic History: New Mexico Geological Society Special Publication, v. 11, p. 1-34.

Lackey, J.S., Valley, J.W., and Saleeby, J.B., 2005, Supracrustal input to magmas in the deep crust of Sierra Nevada batholith: Evidence from high-δ^{18}O zircon: Earth and Planetary Science Letters, v. 235, p. 315-330.

Lackey, J.S., Valley, J.W., Chen, J.H., and Stockli, D.F., 2008, Dynamic magma systems, crustal recycling, and alteration in the central Sierra Nevada batholith: The oxygen isotope record: Journal of Petrology, v. 49, p. 1397-1426.

Matsuhisa Y., 1979, Oxygen isotopic compositions of volcanic rocks from the east Japan island arc and their bearing on petrogenesis: Journal of Volcanology and Geothermal Research, v. 5, p. 271–296.

McIntosh, W.C., Chapin, C.E., Ratté, J.C., and Sutter, J.F., 1992, Time-stratigraphic framework for the Eocene-Oligocene Mogollon-Datil volcanic field, southwest New Mexico: Geological Society of America Bulletin, v. 104, p. 851-871.

McMillan, N.J., 1998, Temporal and spatial magmatic evolution of the Rio Grande rift: New Mexico Geological Society, Guidebook 49, p. 107-116.

McMillan, N.J., Dickin, A.P., and Haag, D., 2000, Evolution of magma source regions in the Rio Grande rift, southern New Mexico: Geological Society of America Bulletin, v. 112, p. 1582-1593.

McMillan, N.J., Mack, G., and Giles, K., 2004, Magmatic record of Laramide subduction and the transition to Tertiary extension: Upper Cretaceous through Eocene igneous rocks of New Mexico, *in* Mack, G.H. and Giles, K.A, eds., The Geology of New Mexico: A Geologic History: New Mexico Geological Society, Special Publication 11, p. 249-270.

Michelfelder, G., Feeley, T., Wilder, A., and Klemetti, E., 2013, Modification of the Continental Crust by Subduction Zone Magmatism and Vice-Versa: Across-Strike Geochemical Variations of Silicic Lavas from Individual Eruptive Centers in the Andean Central Volcanic Zone: Geosciences, v. 3, p. 633-667.

Michelfelder, G.S., and McMillan, N.J., 2012, Geochemistry, origin, and U-Pb zircon ages of the Sierra Cuchillo laccolith, Sierra County, New Mexico: New Mexico Geological Society, Guidebook 63, p. 249-260.

Muehlenbachs K. and Byerly G., 1982, ^{18}O enrichment of silicic magmas caused by crystal fractionation at the Galapagos spreading center: Contributions to Mineralogy and Petrology, v. 79, p. 76–79.

Ramos, F.C., and Reid, M.R., 2005, Distinguishing melting of heterogeneous mantle sources from crustal contamination: Insights from Sr isotopes at the phenocryst scale, Pisgah Crater, California: Journal of Petrology, v. 46, p. 999-1012.

Rentz, S.P., Michelfelder, G.S., Coble, M.A., Salings, E.E., *in press*, U-Pb zircon geochronology of calc-alkaline ash flow tuff units in the Mogollon Datil Volcanic Field, southern New Mexico, *in* Poland, M., Garcia, M., and Grunder, A., eds., Geological Society of America Special Publication.

Sheppard, S.M.F., and Harris, C., 1985, Hydrogen and oxygen isotope geochemistry of Ascension Island lavas and granites: Variation with crystal crystallization and interaction with sea water: Contributions to Mineralogy and Petrology, v. 91, p. 74–81.

Takeuchi, A., and Larson, P.B., 2005, Oxygen isotope evidence for the late Cenozoic development of an orographic rain shadow in eastern Washington, USA: Geology, v. 33, p. 313-316.

Taylor H.P., Jr, 1968, The oxygen isotope geochemistry of igneous rocks: Contributions to Mineralogy and Petrology, v. 19, p. 1-71.

Underwood, S.J., and Clynne, M.A., 2017, Oxygen isotope geochemistry of mafic phenocrysts in primitive mafic lavas from the southernmost Cascade Range, California: American Mineralogist, v. 102, p. 252-261.

Valley, J.W., Kitchen, N., Kohn, M.J., Niendorf, C.R., and Spicuzza, M.J., 1995, UWG-2, a garnet standard for oxygen isotope ratios: Strategies for high precision and accuracy with laser heating: Geochimica et Cosmochimica Acta, v. 59, p. 5223-5231.